J Mater Sci (2007) 42:2387–2392
DOI 10.1007/s10853-006-1277-z

Convection–diffusion derived gradient films on porous substrates and their microstructural characteristics

Yanwei Zeng · Changan Tian · Junliang Liu

Received: 4 August 2005 / Accepted: 30 January 2006 / Published online: 17 December 2006

Abstract By virtue of the convection–diffusion effect of solution in porous solid media, an alumina substrate-supported electrolyte film (YSZ) with gradient microstructure has been successfully fabricated for the first time and structurally characterized by SEM and XRD–ADA (angular dispersion analysis). This novel fabrication technique is simple, controllable, economical and potentially applicable to fabricating electrode-supported gradient electrolyte films for SOFCs. The so-prepared YSZ-film/substrate structures are featured with a dense YSZ film of ~10 μm, a uniform filling layer of ~50 μm just beneath the interface and a successive diffuse layer stretching as deep as ~250 μm within the porous substrate matrix.

Introduction

In recent years, more and more research and commercial interest have been attracted to the intermediate and low temperature solid oxide fuel cells (SOFCs) [1–3]. The significance of reducing the operation temperature lies in great potential technical and economic benefits. First, the cost of SOFCs technology may be dramatically reduced since less expensive materials can be utilized in cells and novel fabrication techniques may be applied to the stack and system assemblage. Moreover, as the operation temperature goes down, the technical problems associated with elevated temperatures will be greatly avoided so as to achieve a pronounced increase in system reliability and durability [4–9].

However, the operation temperature reduction inevitably yields new issues such as the exponential drop in conductivities of cell's materials and the remarkable increase of interfacial polarization resistances between cathode/anode and electrolyte layers. To face these new challenges, two basic strategies have been practiced: (1) searching for novel materials with sufficient ionic conductivity and chemical stability, (2) exploring novel microstructures of cell components by using novel fabrication and processing techniques, such as fabricating supported electrolyte films, developing composite cathodes/anodes with uniform or gradient microstructures, etc. It has been recognized that the oxygen ionic flux could be increased by several times when a normal YSZ electrolyte membrane was thinned from few hundreds to few tens micros at 800 °C. Such an electrolyte film may be built upon the porous cathodes or anodes via vapor phase deposition (VD), electrochemical and vapor phase electrolytic deposition (ECVD and VED), Sol–gel coating techniques, as well as slurry or colloidal deposition, etc [10–16]. It was reported that the interfacial polarization resistance for a LSM/YSZ cathode/electrolyte system might be reduced a great deal by incorporating YSZ or GDC phases into the LSM cathode or using a mixed electronic–ionic conductive material [17, 18]. In these cathode materials, the oxygen ionic transport and electric charge transfer are greatly enhanced due to the presence of more triple phase boundaries or to the

Y. Zeng (✉) · C. Tian · J. Liu
School of Materials Science & Engineering, Nanjing University of Technology, Nanjing 210009, P.R. China
e-mail: zengyanwei@tom.com

coexistence of ionic and electronic conductivities. What is more noteworthy, however, the concept of functionally graded materials (FGM) has been introduced recently to the fabrication of SOFCs components to improve their interfacial conditions and electrochemical performance. Some single-phase cathode materials (e.g. LSM/LSC) and composite cathodes (e.g. LSM/LSC–YSZ/GDC) were prepared on YSZ electrolytes via different methods such as screen printing, slurry-spraying, spray-painting, and slurry coating, resulting in the reduced interfacial polarization resistances and improved electrochemical performances [19–23]. Nonetheless, the works reported in the literature were mostly focused on electrolyte-supported porous cathodes or anodes with compositional gradients. This kind of structures is of a large thickness of electrolytes and therefore disadvantageous for an intermediate temperature SOFCs. According to the modeling investigation of a SOFC's electrochemical performance [24], the best structure for a SOFC with lowered interfacial polarization resistance should consist of a dense electrolyte film with gradient layers stretching into the supporting cathode or anode. The electrolyte/electrode structures of this kind would greatly favor not only the reduction of interfacial polarization resistance but the enhancement of electrode electrochemical reactions as well for both single-phase mixed conductive cathodes and composite cathodes.

In the present paper, we report our recent work on the fabrication of supported dense electrolyte films with gradient structures stretching into a porous alumina substrate via a well-controlled convection–diffusion process of solution. This novel technique is simple, controllable, economical and potentially applicable to the fabrication of electrode-supported electrolyte films for SOFCs.

Fabrication principles and procedures

As schematically shown in Fig. 1, the lab setup for the fabrication of supported dense electrolyte films with gradient structure is a well-designed glass vessel, on which a pre-sintered porous substrate is mounted with its peripheral edge tightly sealed and properly kept in contact with the solution containing volatile solvent (e.g. methanol) and desirable chemical species as solutes. The vertical glass tube connected to the vessel is used to form a height of liquid column so as to control the liquid pressure at the bottom of the substrate. Under the hydraulic pressure of liquid, the solution immediately penetrates into the porous plate and flows upwards as

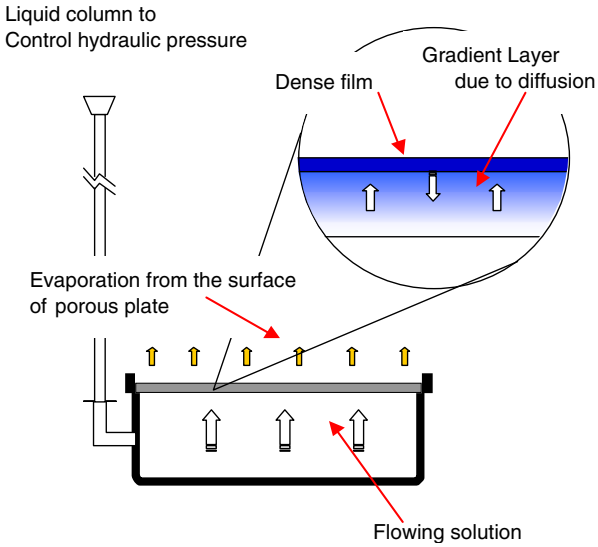

Fig. 1 The schematic of lab setup for fabricating supported electrolyte thin films with gradient porous structure

convection. When the solution reaches top surface of the substrate, the solvent evaporation occurs, leaving the solute species at the surface and resulting in a higher concentration of species in the surface area than elsewhere in the system, which in turn provokes a diffusion of the species in the direction opposite to the convection. Therefore, the convection or micro-flow inside the porous substrate driven by the hydraulic pressure of liquid column brings the solution upwards while the diffusion driven by the concentration gradient pushes the solute downwards. As a final result, the overall consequence is the formation of a diffusing concentration profile with a peak at top surface of the substrate. Moreover, such a diffusion concentration profile can be properly controlled by adjusting the height of liquid column and the evaporation rate of solvent.

In the experiment, the porous well-sintered alumina plates were used as substrates. They were 30 mm in diameter, 1.5 mm in thickness and of a porosity of 40 ± 1% (measured by Hg-porosimetry) and obtained by conventional ceramic technique from alumina powder of ~1 μm in diameter. For each plate, one surface was well polished and cleaned for the growth of electrolyte thin film. The solutions were prepared with methanol as solvent at various concentrations (0.1–0.2 M) of zirconium chloride plus yttrium chloride in a stoichiometry of 8 mol% Y_2O_3–ZrO_2 (YSZ).

The solvent evaporation and gradient structure formation were conducted in a ventilation cabinet at room temperature. In order to adjust the evaporation rate of solvent, an infrared bulb of 500 W was used and the irradiation on the growth surface was controlled by

adjusting vertical distance from the growth surface to the bulb. During the experiments, the evaporation surface of liquid was carefully controlled just at top surface of the alumina plates all the time by timely adjusting the height of liquid column. After a predetermined evaporation was fulfilled, the solution in the glass vessel was replaced with pure methanol and a similar evaporation was carried out for 2 more hours to rinse the pore channels inside the structure and enhance the gradient distribution of precipitated species in the plate's surface area.

The so-prepared electrolyte/substrate samples were first dried at 100 °C for 2 h and then fired at 1,350 °C for 2 h for the densification of films. Their microstructural features were characterized using a scanning electron microscope (SEM, JSM-5900) and an X-ray diffractometer (XRD-X'TRA) for the quantitative profile analysis of gradient structure.

Results and discussions

Solvent evaporation

During the experiment, it was observed that when the solution concentration and infrared irradiation were given, the methanol evaporation quantity per unit surface area (μg/mm^2) invariably went down quickly in the initial stage and then gradually to a very small value as the time increased. Several typical evaporation rate–time curves under different evaporation conditions were presented in Fig. 2. It can be noted that an intensive infrared irradiation causes a higher evaporation rate in the initial stage but a lower one afterwards. As to the influence of solution concentration, the increased concentration appears to remarkably reduce evaporation rate all the time, especially in the initial stage. Such a methanol evaporation behavior can be mainly attributed to the microflow of solution in the pores of substrates when the evaporation surface of liquid is controlled at the surface. As the evaporation goes on, the micropores in the surface area of substrate tend to become narrower and narrower due to the accumulation and precipitation of solute species. As a result, the flow resistance of liquid in the pores inevitably increases and the effective evaporation surface area is decreased. Therefore, it can be inferred that the apparent evaporation rate of methanol is dynamically controlled by the pore-filling process within the porous substrates. It should be the convoluted result of solution convection, solute species diffusion, accumulation and precipitation, which eventually determine the profiles of precipitation across the thickness of substrates. For more detailed analyses and discussions, a mathematical modeling of the processes is needed. This work has been fulfilled and the results are to be published elsewhere.

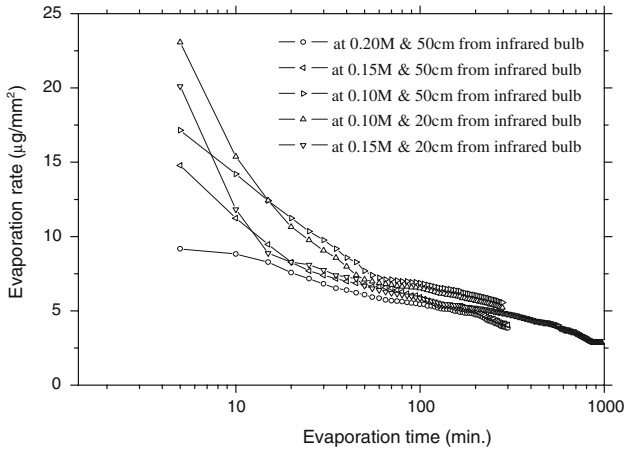

Fig. 2 Representative evaporation rate–time dependences under different experimental conditions

Profile structural analyses

The typical SEM images of YSZ electrolyte/substrates fabricated in our method are shown in Fig. 3. It can be seen that a dense YSZ electrolyte film was formed on the alumina substrate (see Fig. 3a, b). It measures ~10 μm in thickness, depending on the fabricating conditions such as concentration of solution, evaporation rate, temperature and time length, etc. The interface between YSZ film and substrate can be observed, beneath which a diffuse layer of YSZ is identified in contrast to the porous alumina matrix (see Fig. 3c, d). According to the back scanning images, it has been estimated that the uniform layer of YSZ inside porous alumina matrix arrives at ~50 μm but the total diffuse depth of YSZ reaches ~250 μm.

To quantitatively understand gradient microstructure of the YSZ electrolyte films in porous alumina substrates, an X-ray angular dispersion analysis (ADA) has been performed with the samples beside the conventional XRD analyses. In the experiment, the X-ray tube was set to move in step mode from 0° to 30° for the angle α between the incident bean and the sample surface, while the detector was fixed at $2\theta = 30°$ to receive the reflection bean from (111) plane of cubic YSZ, with the diffraction geometry schematically illustrated in Fig. 4.

A representative conventional XRD pattern of the samples is shown in Fig. 5. It clearly indicates that together with the X-ray diffraction peaks of cubic YSZ

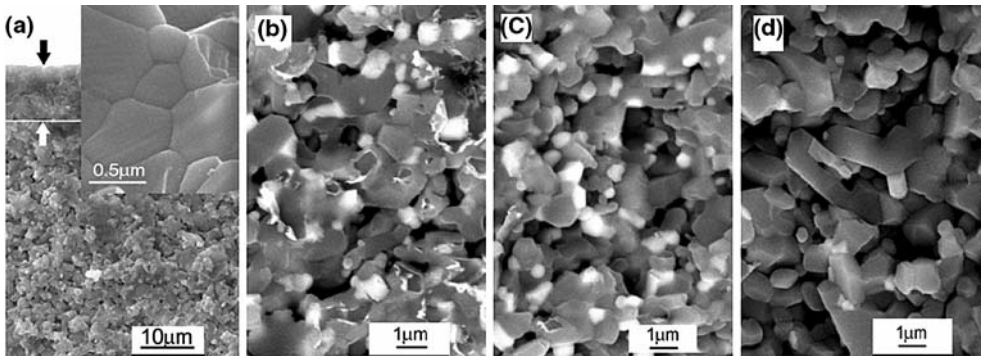

Fig. 3 Typical SEM micrographs of the cross-sections of supported YSZ electrolyte film with gradient structure stretching into the porous substrate. (**a**) An overview at low magnification (the inset showing the well sintered film); (**b**) local view just beneath the interface; (**c**) away from the interface; (**d**) far away from the interface

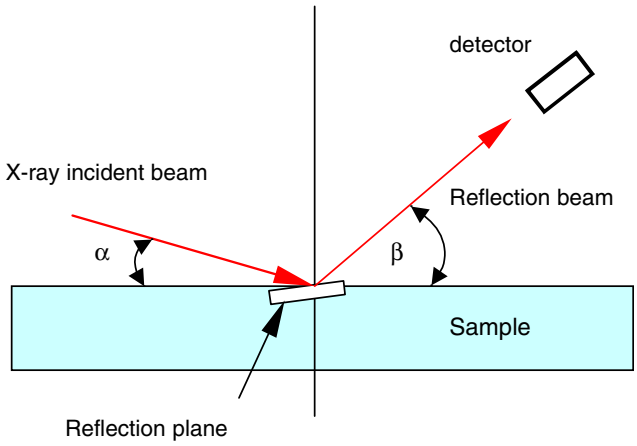

Fig. 4 X-ray diffraction geometry for angular dispersion analysis (ADA)

(despite of a few bud-like reflections for trace quantity of monoclinic phase), the diffraction peaks of α-alumina phase were also well identified, suggesting that the X-ray intensity was high enough to penetrate the surface layer and enter into the porous alumina substrate for a 2θ-scan from 10 to 80°. Therefore, the diffraction intensity of YSZ phase should comprise two contributions, one from the top dense YSZ film and the other from the underlying gradient YSZ layer in porous substrate.

Figure 6 shows an X-ray ADA diffraction pattern with respect to the strongest reflection from plane (111) for YSZ. It can be seen that the ADA diffraction intensity curve as a function of X-ray incident angle α is quite symmetrical about the central position at $\alpha = 15°$, indicating no remarkable preferred plane orientation in the sample. It appears to grow first gradually then ever-increasingly as the angle α increases from zero. Such a behavior is theoretically dominated by X-ray effective penetration depth and the real distribution of YSZ phase that diffracts X-ray. Clearly, in the regime of low angle (a few degree), the X-ray penetration is quite shallow and the diffraction should mainly occur in the dense YSZ film. As the angle α increases, the YSZ phase located at greater depth will contribute more and more to the total diffraction intensity.

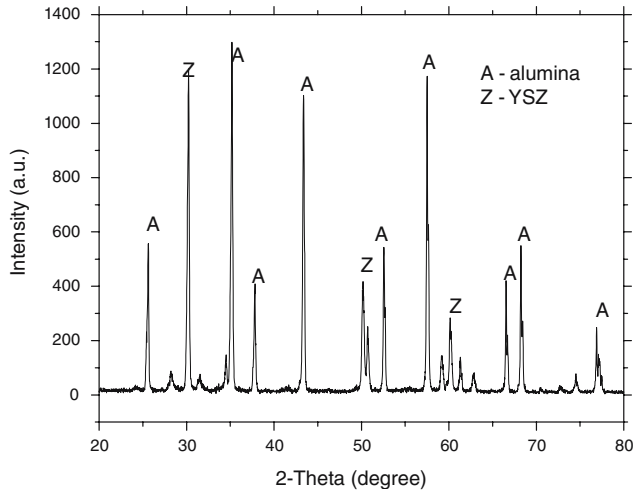

Fig. 5 Conventional XRD pattern of an YSZ/alumina gradient film structure

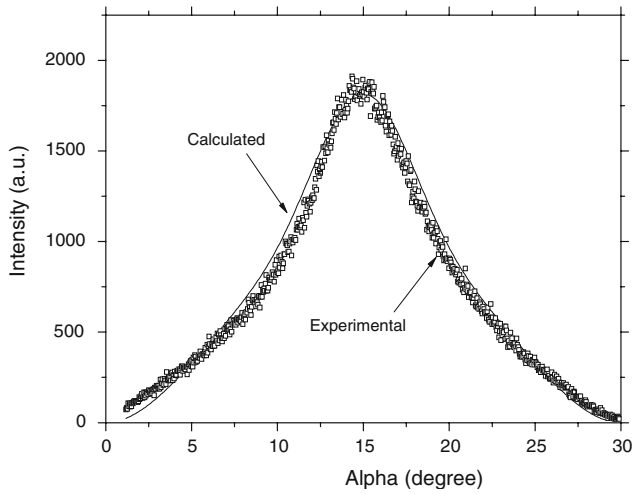

Fig. 6 XRD pattern of an YSZ/alumina for ADA with 2θ = 30° and α scanning from 2 to 30°

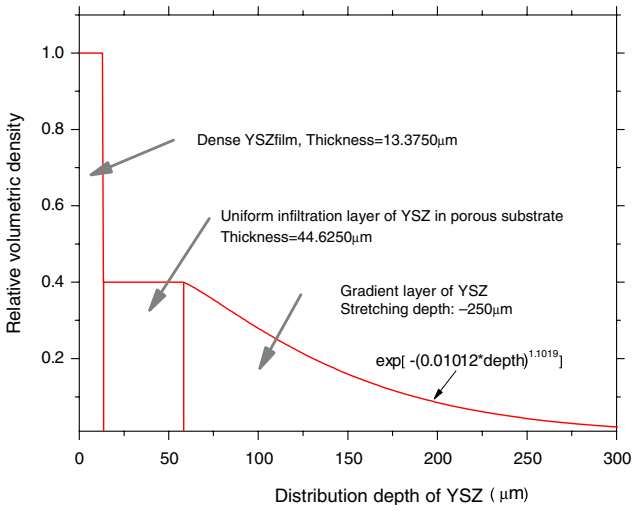

Fig. 7 Relative density distribution of YSZ on and across the porous substrate

To realize a quantitative analysis, the present YSZ/alumina gradient structure is assumed to be composed of three layers: (1) dense YSZ film, (2) YSZ-filled layer and (3) YSZ-diffused layer. In terms of the X-ray absorption principles [25, 26], the diffraction intensity for a given crystal plane k in such a microstructure can be written as:

$$I_k(\alpha) = K \int_{\Omega} \rho_k \exp\left[-\mu(z) z \left(\frac{\sin\alpha + \sin\beta}{\sin\alpha \sin\beta}\right)\right] \mathrm{d}v \qquad (1)$$

where K is a proportional constant, $\beta = 2\theta - \alpha$ and Ω denotes the effective diffraction volume, over which the integration is performed. The parameters ρ_k and $\mu(z)$, as a function of profile depth z in the present case, are, respectively, the volumetric density of the crystal plane k and X-ray linear absorption coefficient. On the basis of the above-mentioned three-layer model, they may be simply described by the following equations:

$$\rho_k \propto \begin{cases} \rho_0, & 0 \le z \le t_1 \\ \rho_0 v, & t_1 < z \le t_2 \\ \rho_0 v e^{-az^b}, & t_2 < z \end{cases} \qquad (2a)$$

$$\mu = \begin{cases} \mu_{\mathrm{YSZ}} & 0 \le z \le t_1 \\ \mu_{\mathrm{YSZ}} v + \mu_{\mathrm{Sub}}(1-v) & t_1 < z \le t_2 \\ \mu_{\mathrm{YSZ}} v \exp(-az^b) + \mu_{\mathrm{Sub}}(1-v) & t_2 < z \end{cases} \qquad (2b)$$

with ρ_0 denoting the real density of YSZ, v the volume fraction of pores in the alumina substrate, a and b are two parameters for describing the gradient distribution of YSZ in the substrate.

Using Eqs. 1 and 2, a computer numerical analysis of the experimental X-ray diffraction data was carried out through a curve-fitting. As the best-fitting result, the fitting curve of the experimental data is shown in Fig. 6 and the corresponding parameters were evaluated with t_1 = 13.3750 μm (dense YSZ film), t_2 = 44.6250 μm (uniform YSZ-filled layer) and $a = 1.0120 \times 10^{-2}$/μm, b = 1.1019 (for gradient layer), respectively. These data define a laminated and graded microstructure of YSZ/alumina structures with a particular profile depicted as shown in Fig. 7, which is quite consistent with the results from SEM image analysis.

Conclusions

The supported electrolyte films (8-YSZ) with gradient microstructures rooted in porous alumina substrates have been successfully fabricated by means of convection–diffusion effect of solution in porous solid media. The so-prepared supported YSZ-film/substrate structures, as manifested by SEM and XRD–ADA (angular dispersion analysis), are featured with a dense YSZ film of ~10 μm, a uniform filling layer of ~50 μm just beneath the interface and a successive diffuse layer stretching as far as ~250 μm within the porous substrate matrix. This novel technique is simple, controllable, economical and potentially applicable to fabricating electrode-supported gradient electrolyte films for planar SOFCs.

Acknowledgements The financial support from the Committee for Science and Technology of Jiangsu, P.R. China through Grant BK2002018, 2002 is gratefully acknowledged.

References

1. Lu C, An S, Worrell WL, Vohs JM, Gorte RJ (2004) Solid State Ionics 175:47
2. Zha SW, Rauch W, Liu ML (2004) Solid State Ionics 166:241
3. Leng YJ, Chan SH, Jiang SP, Khor KA (2004) Solid State Ionics 170:9
4. Park S, Vohs JM, Gorte RJ (2000) Nature 404:265
5. Schiller G et al (2000) Proceedings of the 4th European SOFCs Forum, vol 37
6. Steele BCH (2000) Solid State Ionics 129:95
7. de Souza S, Visco SJ, Dejonghe LC (1997) J Electrochem Soc 144:L35
8. Singhal SC (2002) Solid State Ionics 152:405
9. Suzuki T, Kosacki I, Anderson HU (2002) Solid State Ionics 151:111
10. Akiyama Y, Imaishi N, Shin YS, Jung SC (2002) J Cryst Growth 241:352
11. Di Giuseppe G, Selman JR (2001) J Mater Res 16:2983
12. Uchimoto Y, Tsutsumi K, Ioroi T, Ogumi Z (2000) J Am Ceram Soc 83:77

13. Kueper TW, Visco SJ, De Jonghe LC (1992) Solid State Ionics 52:251
14. Stech M, Reynders P, Rodel J (2000) J Am Ceram Soc 83:1889
15. Will J, Hruschka HKM, Gubler L, Gauckler LJ (2001) J Am Ceram Soc 84:328
16. De Jonghe LC, Jacobson CP, Visco SJ (2003) Annu Rev Mater Res 33:169
17. Kenjo T, Nishiya M (1992) Solid State Ionics 57:295
18. Murray EP, Barnett SA (2001) Solid State Ionics 143:265
19. Herbstritt D et al (1999) Electrochem Soc 99(19):972
20. Hart NT, Brandon NP, Day MJ, Shemilt JE (2001) J Mater Sci 36:1077
21. Hart NT, Brandon NP, Day MJ, Lapena-Rey N (2002) J Power Sources 106:42
22. Holtapples P, Bagger C (2002) J Eur Ceram Soc 22:41
23. Xia C, Rauch W, Wellborn W, Liu M (2002) Electrochem Solid State Lett 5:A217
24. Zeng YW, Tian CA, Bao LM (2005) J Power Sources 139:35
25. Warren BE (1969) X-ray diffraction. Addison-Wesley publishing Company
26. Chong QZ (1997) Polycrystalline two-dimensional x-ray diffraction. Science Press (China)